

AD-A170 227

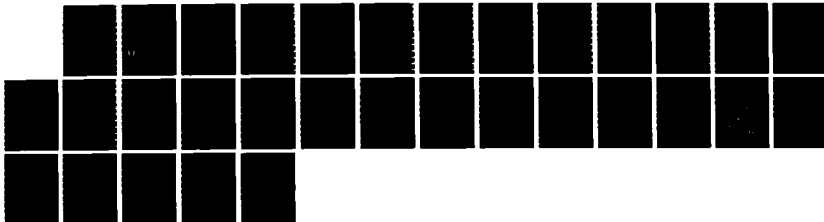
SIMULATION FATIGUE TESTING OF AN AUTOFRETTAGED CYLINDER 1/1
WITH AN OUTSIDE D. (U) ARMY CLOSE COMBAT ARMAMENTS
CENTER WATERVLIET NY J A KAPP ET AL. JUN 86

UNCLASSIFIED

ARCCB-TR-86022

F/G 13/9

NL





1.0



1.1



1.25



1.4



1.6

5.0
5.6
6.3
7.1
8.0
9.0
10.0

2.8



2.5

3.15



2.2

3.5



2.0

4.0



1.8

4.5



1.6

12

AD

TECHNICAL REPORT ARCCB-TR-86022

SIMULATION FATIGUE TESTING OF AN AUTOFRETTAGED CYLINDER WITH AN OUTSIDE DIAMETER NOTCH: THE EFFECTS OF ROOT RADIUS AND SURFACE CONDITION PART 1 -VERY LOW CYCLE APPLICATIONS

AD-A170 227

J. A. KAPP
V. P. GRECO
R.T. ABBOTT

DTIC
ELECTE
JUL 23 1986
B

JUNE 1986



**US ARMY ARMAMENT RESEARCH AND DEVELOPMENT CENTER
CLOSE COMBAT ARMAMENTS CENTER
BENET WEAPONS LABORATORY
WATERVLIET, N.Y. 12189-4050**

DTIC FILE COPY

APPROVED FOR PUBLIC RELEASE; DISTRIBUTION UNLIMITED

86 7 28 118

DISCLAIMER

The findings in this report are not to be construed as an official Department of the Army position unless so designated by other authorized documents.

The use of trade name(s) and/or manufacturer(s) does not constitute an official indorsement or approval.

DESTRUCTION NOTICE

For classified documents, follow the procedures in DoD 5200.22-M, Industrial Security Manual, Section II-19 or DoD 5200.1-R, Information Security Program Regulation, Chapter IX.

For unclassified, limited documents, destroy by any method that will prevent disclosure of contents or reconstruction of the document.

For unclassified, unlimited documents, destroy when the report is no longer needed. Do not return it to the originator.

REPORT DOCUMENTATION PAGE		READ INSTRUCTIONS BEFORE COMPLETING FORM
1. REPORT NUMBER ARCCB-TR-86022	2. GOVT ACCESSION NO. AD-A170 227	3. RECIPIENT'S CATALOG NUMBER
4. TITLE (and Subtitle) SIMULATION FATIGUE TESTING OF AN AUTOFRETTAGED CYLINDER WITH AN OUTSIDE DIAMETER NOTCH: THE EFFECTS OF ROOT RADIUS AND SURFACE CONDITION PART I - VERY LOW CYCLE APPLICATIONS	5. TYPE OF REPORT & PERIOD COVERED Final	
	6. PERFORMING ORG. REPORT NUMBER	
7. AUTHOR(s) J. A. Kapp, V. P. Greco, and R. T. Abbott	8. CONTRACT OR GRANT NUMBER(s)	
9. PERFORMING ORGANIZATION NAME AND ADDRESS US Army Armament Research, Develop, & Engr Center Benet Weapons Laboratory, SMCAR-CCB-TL Watervliet, NY 12189-4050	10. PROGRAM ELEMENT, PROJECT, TASK AREA & WORK UNIT NUMBERS AMCMS NO. 2080.18.6000.000 PRON NO. 1A3223B91A1A	
11. CONTROLLING OFFICE NAME AND ADDRESS US Army Armament Research, Develop, & Engr Center Close Combat Armaments Center Dover, NJ 07801-5001	12. REPORT DATE June 1986	
	13. NUMBER OF PAGES 22	
14. MONITORING AGENCY NAME & ADDRESS (if different from Controlling Office)	15. SECURITY CLASS. (of this report) Unclassified	
	15a. DECLASSIFICATION/DOWNGRADING SCHEDULE	
16. DISTRIBUTION STATEMENT (of this Report) Approved for public release; Distribution unlimited		
17. DISTRIBUTION STATEMENT (of the abstract entered in Block 20, if different from Report)		
18. SUPPLEMENTARY NOTES Presented at ASME Pressure Vessel Conference, New Orleans, LA, 24-28 June 1986 To be published in the Journal of Pressure Vessel Technology		
19. KEY WORDS (Continue on reverse side if necessary and identify by block number) Fatigue Life Notch Root Radius Thick-Wall Cylinder Crack Initiation Ball Peening		
20. ABSTRACT (Continue on reverse side if necessary and identify by block number) The effects of notch root radius, electropolishing after machining, and glass ball peening after machining have been studied in simulation tests of an outside diameter (OD) notched, autofrettaged thick-walled cylinder subjected to cyclic internal pressure. Fatigue life measurements were made using specimens designed such that the stress at the notch root due to both autofrettage and pressure were simulated exactly. Fatigue life was defined as the number of (CONT'D ON REVERSE)		

TABLE OF CONTENTS

	<u>Page</u>
INTRODUCTION AND PROBLEM STATEMENT	1
EXPERIMENTAL PROCEDURE	2
STRESS ANALYSIS	4
LOCAL STRAIN LIFE ESTIMATE	6
RESULTS AND DISCUSSION OF RESULTS	7
CONCLUSIONS	11
REFERENCES	12

TABLES

I. STRESS ANALYSIS RESULTS	14
II. ESTIMATED LIFE USING LOCAL STRAIN ANALYSIS	15
III. MEASURED LIVES USING THE SIMULATION SPECIMEN	16

LIST OF ILLUSTRATIONS

1. Sectored thread end connection geometry.	17
2. Simulation specimen.	18
3. Finite element models.	19
4. Strain-life property of the steel tested.	20
5. Crack growth rates as a function of R for the steel tested.	21
6. Measured crack initiation life as a function of notch root radius.	22

INTRODUCTION AND PROBLEM STATEMENT

Some ultra high pressure vessels use threaded connectors as end enclosures. Furthermore, it is sometimes necessary to remove the end enclosure quickly, thus, the sectored thread, Figure 1, has been developed. With this design, the end cap can be removed with only a single one-quarter turn rather than several turns. When it is necessary to maximize the load bearing capability of the connection, the thread area must be maximized and generous root radii at the ends of the thread sectors are not possible. This report summarizes the results of a simulation fatigue test program to evaluate the effects of small root radius and surface treatment on the fatigue crack initiation life.

The vessel in consideration has four sectors and the dimension of the root radius is 0.010 in. R min (0.254 mm R min) to 0.020 in. R max (0.508 mm R max). The material was pressure vessel steel ASTM A723 Grade 1 Class 4 with nominal yield strength of 170 ksi (1172 MPa). The inner diameter (ID) was 5.165 in. (1.31 cm), the major outer diameter (OD) ($2b_1$) was 8.75 in. (22.2 cm), and the minor OD ($2b_2$) was 8.41 in. (21.4 cm). The cylinder was designed to contain 72 ksi (496 MPa) internal pressure and was swage autofrettaged to produce the 100 percent overstrain condition.

Three different treatments of the notch root radius were studied. First, milling to the required dimensions with a faced cutting tool; second, milling followed by electropolishing to both increase the root radius somewhat and to produce a smoother surface finish; and third, milling followed by glass ball peening. Steel shot could not be used because of the very small root radius.

An earlier study (ref 1) has shown that electropolishing a grooved sample can substantially increase fatigue life. The as-machined grooves were loaded in a zero-to-tension manner such that failure occurred in about 20,000 cycles. Applying the same loads to samples that had been machined and electropolished increased fatigue life to about 35,000 cycles. This increase was attributed to the removal of material damaged during machining by the electropolishing process. Although the problem considered here is quite different (a tension-tension loading and much lower life), electropolishing is worthy of investigation at this time.

EXPERIMENTAL PROCEDURE

Previous studies (refs 2,3) have shown that adequate simulation of OD initiated failures can be obtained by using the specimen shown in Figure 2. The basic assumption made in using this specimen is that crack initiation occurs at the notch due to local stresses regardless of how the stresses are produced. With the simulation specimen, both the tensile residual stress and the alternating stress due to internal pressurization can be applied by adjusting the load P.

¹V. P. Greco and B. L. Pennell, "Low Cycle Notched-Fatigue Behavior of Broached and Electrochemically Treated Steels (Electropolishing and Chromium Plating)," presented at the 56th Annual Convention, American Electroplater's Society, Detroit, MI, June 1969.

²J. A. Kapp and J. H. Underwood, "Service Simulation Tests to Determine the Fatigue Life of Outside-Diameter-Notched Thick-Wall Cylinder," Experimental Mechanics, Vol. 22, No. 3, March 1982, pp. 96-100.

³J. H. Underwood, "Fatigue Life Analysis and Tensile Overload Effects With High Strength Steel Notched Specimens," High Pressure in Science and Technology, Part II: Fluids, Engineering, and Safety, Vol. 22, 1984, pp. 209-214.

The former investigations modeled a somewhat different OD notch configuration that was substantially deeper than the problem considered here. In those cases, the crack achieved critical size immediately upon initiation in both the pressure loading and simulation loading conditions. Thus, the fatigue crack initiation life was determined as the number of cycles-to-failure. The cylinder we studied is somewhat different. Autofrettage and internal pressurization would result in failure shortly after crack initiation, but the simulation specimen can accommodate large amounts of subcritical crack growth. To alleviate this discrepancy, a small flat was produced on the ID of the simulation specimen directly in line with the OD notch. An ultrasonic probe was placed there to monitor crack initiation. Cycling proceeded until a crack about 0.05 in. (1.3 mm) deep was observed. This depth was chosen because it was the minimum depth that could be reliably detected. Once the crack was indicated, the notch was cut from the specimen and broken apart to reveal the fracture surface. The depth of the fatigue crack was then measured.

The fatigue crack initiation life was determined by calculating the number of cycles necessary for the crack to grow the measured amount. The calculated cycles were then subtracted from the total measured cycles. This calculation was based on the assumption that once the crack initiates, it has dimensions equal to the notch depth ($b_1 - b_2$), and the simulation specimen acts as a solid unnotched ring with the OD equal to $2b_1$. Stress intensity factors for the smooth ring subject to the imposed loading were known from Gross and

Srawley (ref 4), and crack growth rates were determined in a companion study.

STRESS ANALYSIS

The basic prerequisite of the simulation tests is to produce the same stress in the root of the notch by simulation loading as that which occurs in the autofrettaged and pressurized cylinder. This was accomplished by using finite element stress analysis for one notch configuration, and a Neuber diagram (ref 5). The finite element results for the single notch configuration were used to determine the relative error in the Neuber estimate for the same configuration, which was applied to the remaining Neuber results. The stress concentration factors determined this way were used to estimate crack initiation life using a "local strain" method discussed below.

Three loading conditions were evaluated which required two finite element models. Internal pressure and autofrettage loading were studied using the finite element mesh in Figure 3(a) and simulation loading was analyzed with the mesh shown in Figure 3(b). The smaller mesh was used for pressure and autofrettage loading because of the eightfold symmetry of the cylinder. There are no planes of symmetry in the simulation specimen; the entire structure must be studied. The refinement of the meshes around the root radius is shown in Figure 3(c).

⁴B. Gross and J. E. Srawley, "Analysis of Radially Cracked Ring Segments Subject to Forces and Couples," ASTM STP 632, American Society for Testing and Materials, 1977, pp. 39-56.

⁵A. C. Ugural and S. K. Fenster, Advanced Strength and Applied Elasticity, American Elsevier, New York, 1975, p. 83.

The analysis was conducted using cubic isoparametric elements in the APES finite element program (ref 6). Because these powerful elements were used, a relatively coarse mesh was possible. For pressure and autofrettage, 166 nodes were used and for the simulation specimen, 229 nodes were necessary. It is estimated that to obtain equivalent accuracy using constant strain elements, about 4000 degrees of freedom would be necessary for the pressure and autofrettage loading and about 5500 degrees of freedom would be required for the simulation specimen (ref 6).

The loading of these models is straightforward except for the autofrettage case. The residual stresses were simulated using the thermal loading analogy of Hussain et al (ref 7). It was noted in Reference 7 that autofrettage residual stresses have exactly the same distribution as if the cylinders were subjected to a logarithmically varying axisymmetric temperature distribution in the same smooth cylinder. By loading a notched finite element model with the same temperature distribution as that which produces 100 percent overstrain in a smooth cylinder with an OD of $2b_1$, the effects of the notch on the residual stresses can be accurately determined (refs 7,8).

⁶I. N. Gifford, Jr., "APES - Second Generation Two-Dimensional Fracture Mechanics and Stress Analysis by Finite Elements," Report 4799, Naval Ship Research and Development Center, 1979.

⁷M. A. Hussain, S. L. Pu, J. D. Vasilakis, and G. P. O'Hara, Journal of Pressure Vessel Technology, Vol. 102, No. 3, 1980, p. 314.

⁸S. L. Pu and M. A. Hussain, Journal of Pressure Vessel Technology, Vol. 103, May 1981, p. 301.

LOCAL STRAIN LIFE ESTIMATE

Accurate predictions of the fatigue life of notched components have been made using the "local strain" method (ref 9). This technique works as follows: the strain range ($\Delta\epsilon$) and strain ratio ($R = \epsilon_{\min}/\epsilon_{\max}$) at the root of the notch are estimated using an elastic analysis of the specimen. Crack initiation life is estimated from the steel strain-life property generated by using strain-controlled loading, and by accounting for the effects of R. The equivalent local strain range was calculated by

$$\Delta\epsilon = k_f \frac{(\sigma_{\min} - \sigma_{\max})}{E} \quad (1)$$

and the strain ratio was

$$R = \sigma_{\min}/\sigma_{\max} \quad (2)$$

Where k_f is the fatigue stress concentration factor which is related to the static elastic stress concentration factor k_t for this material by (ref 9):

$$k_f = 1 + q(k_t - 1) \quad (3)$$

$$q = \frac{1}{1 + \bar{a}/\rho} \quad (4)$$

$$\bar{a} = 0.001 \left(\frac{300}{\sigma_u} \right)^{1.8} \quad (5)$$

$$\bar{a} = 0.0254 \left(\frac{2078}{\sigma_u} \right)^{1.8} \quad (6)$$

⁹H. S. Reemsnyder, "Constant Amplitude Fatigue Life Assessment Models," SAE Technical Paper Series 820688, Proceedings of the SAE Fatigue Conference, April 1982, pp. 119-132.

where σ_u is the ultimate tensile strength of the material in units of ksi in Eq. (5) or in units of MPa in Eq. (6).

RESULTS AND DISCUSSION OF RESULTS

The stress analysis results are summarized in Table I. The stress concentration factors (k_t) determined from the finite element models for each loading condition with the minimum root radius are reported. Also, k_t for several notch geometries within the tolerance are given from a Neuber diagram. As can be seen the agreement is quite good, but the finite element results are somewhat lower than that predicted by the Neuber diagram. Since the Neuber diagram gives an estimated k_t for a geometry that is somewhat different than the actual cylinder, it is assumed that the finite element results are more accurate and should be used in subsequent analyses. As k_t is not a constant with respect to loading condition, an average was determined from the finite element solutions. This appears in the final column of the Table I.

To estimate k_t for the more generous root radii, it was decided to use only the Neuber diagram. The finite element solutions were too time consuming. To improve the accuracy of the Neuber diagram, a ratio was established from the one condition in which both finite element and Neuber results were available. This ratio was then multiplied by the k_t estimated from the Neuber diagram. These values of k_t appear as the final column in the table as a function of root radius.

The k_t values determined in this manner were used to estimate the life of the notched cylinder using the local strain concepts. Equations (4) and (5) were used along with other information given in Table II to generate first k_f ,

then the estimated local strain range. These are also given in Table II. Knowing both the strain range and the strain ratio, an estimate of the number of cycles to initiate a crack can be made with the help of Figure 4. The ϵ -N curve for the same material tested here was generated previously in a companion study, as was the crack growth rate as a function of stress intensity factor range and R (Figure 5). The number of cycles necessary to initiate a crack are given in the final column of Table II. These results seem as expected, namely as the root radius increases, the local loading is less severe and longer lives should be observed.

The measured fatigue lives of the specimens tested are summarized in Table III. In this table all of the information gathered on the simulation specimen is given: the measured root-radius (ρ), the measured length of the fatigue crack that developed (Δc), the total number of cycles accumulated when the test was terminated (N_t), the calculated number of cycles to propagate a crack to that depth ($N_{\Delta c}$), and the estimated number of cycles to initiation ($N_i = N_t - N_{\Delta c}$). $N_{\Delta c}$ was determined with the help of Figure 5 and the stress intensity factors for a curved bar with an external crack subject to combined bending and compression (ref 4). As stated above, it was assumed that at initiation, the simulation specimen acts as a smooth curved specimen with an external crack. Its dimensions were assumed to be: OD = $2b_1 = 8.75$ in. (22.2 cm), ID = 5.17 in. (13.12 cm), and crack length $c = b_1 - b_2 = 0.17$ in.

⁴B. Gross and J. E. Srawley, "Analysis of Radially Cracked Ring Segments Subject to Forces and Couples," ASTM STP 632, American Society for Testing and Materials, 1977, pp. 39-56.

(0.43 cm). From Reference 4, it was found that the stress intensity factor range (ΔK) for this initial condition was about $49 \text{ ksi}\sqrt{\text{in.}}$ ($54 \text{ MPa}\sqrt{\text{m}}$). After as much as 0.070 in. (0.18 cm) of crack extension, ΔK was about $52 \text{ ksi}\sqrt{\text{in.}}$ ($57 \text{ MPa}\sqrt{\text{m}}$). Since ΔK changed little, small errors were incurred when the cycles to extend the crack were calculated as $N_{\Delta c} = \Delta c / (dc/dN(\Delta K = 50.5 \text{ ksi}\sqrt{\text{in.}}))$, ($55.5 \text{ MPa}\sqrt{\text{m}}$). From Figure 5 at $\Delta K = 50.5 \text{ ksi}\sqrt{\text{in.}}$ ($55.5 \text{ MPa}\sqrt{\text{m}}$) and $R = +0.5$, $dc/dN \approx 2.1 \times 10^{-4} \text{ in./cycle}$ ($5.3 \times 10^{-6} \text{ m/cycle}$). The calculated values of $N_{\Delta c}$ were small and probably very approximate because of the assumptions made. If more were known of the growth of small fatigue cracks near a notch, a better estimate of $N_{\Delta c}$ could be made. Although the values reported in the table are only estimates, they are still reported to account for the fact that the fracture surfaces showed fatigue cracks of different lengths and certainly some number of cycles were necessary to grow the cracks.

The data are further compared graphically in Figure 6. From this figure we see that the local strain life estimate gives a lower bound of the measured behavior, especially with the larger root radii. The model can underestimate life by as much as 50 percent in the as-machined samples. This difference can be attributed to scatter. The important observation to make from this plot is that changing the root radius will affect fatigue crack initiation life more than surface treatment. For example, local strain analysis suggests that the life to initiate a crack at a notch with a root radius of 0.020 in.

⁴B. Gross and J. E. Srawley, "Analysis of Radially Cracked Ring Segments Subject to Forces and Couples," ASTM STP 632, American Society for Testing and Materials, 1977, pp. 39-56.

(0.508 mm) should be about twice as long as to initiate a crack with a root radius of 0.010 in. (0.254 mm). The experimental data shows that a somewhat greater ratio is obtained. Comparing specimens 18 and 9 with root radii of 0.012 in. (0.305 mm) and 0.018 in. (0.457 mm) respectively, life was increased by more than a factor of three. The data from the electropolished samples cannot be distinguished from the as-machined samples, nor can the glass peening results be interpreted as improving fatigue life. This relative insensitivity of fatigue life to notch surface condition is in agreement with prior results (ref 3), of fatigue life tests with notch root stresses greatly in excess of the yield strength. There was one electropolished sample (specimen no. 2) that indeed indicated an improvement, but since that result could not be repeated, it was assumed to be an artifact and inconclusive.

Although the results of changing surface treatments were ineffective in this case, we cannot generalize these results. We tested under only one loading condition resulting in a very low life. It is clear that under the conditions studied, any effect due to either electropolishing or glass ball peening were overcome by the substantial inelastic behavior at the root radius. It is well known that peening increases fatigue life in the high cycle regimen and previous studies (ref 1) also indicate the same for electropolishing.

¹V. P. Greco and B. L. Pennell, "Low Cycle Notched-Fatigue Behavior of Broached and Electrochemically Treated Steels (Electropolishing and Chromium Plating)," presented at the 56th Annual Convention, American Electroplater's Society, Detroit, MI, June 1969.

³J. H. Underwood, "Fatigue Life Analysis and Tensile Overload Effects With High Strength Steel Notched Specimens," High Pressure in Science and Technology, Part II: Fluids, Engineering, and Safety, Vol. 22, 1984, pp. 209-214.

CONCLUSIONS

The low cycle fatigue crack initiation life of an autofrettaged cylinder with a notch on its OD can be adequately determined with a simulation specimen if care is taken to detect crack initiation. The effects of the root radius of the notch can be easily determined experimentally with this technique. The result is that increasing the root radius from about 0.010 in. (0.254 mm) to about 0.020 in. (0.508 mm) increases the initiation life by about a factor of three. Whether the cylinder is cycled as-machined, or followed by electro-polishing or glass ball peening, there is no effect on fatigue crack initiation life. Further testing with higher life cylinders should be performed to assess the effects of surface treatments more thoroughly. Finally, the lower bound of fatigue initiation life can be determined using local strain analysis, if smooth specimen strain range versus cycles-to-failure data are available.

REFERENCES

1. V. P. Greco and B. L. Pennell, "Low Cycle Notched-Fatigue Behavior of Broached and Electrochemically Treated Steels (Electropolishing and Chromium Plating)," presented at the 56th Annual Convention, American Electroplater's Society, Detroit, MI, June 1969.
2. J. A. Kapp and J. H. Underwood, "Service Simulation Tests to Determine the Fatigue Life of Outside-Diameter-Notched Thick-Wall Cylinder," Experimental Mechanics, Vol. 22, No. 3, March 1982, pp. 96-100.
3. J. H. Underwood, "Fatigue Life Analysis and Tensile Overload Effects With High Strength Steel Notched Specimens," High Pressure in Science and Technology, Part II: Fluids, Engineering, and Safety, Vol. 22, 1984, pp. 209-214.
4. B. Gross and J. E. Srawley, "Analysis of Radially Cracked Ring Segments Subject to Forces and Couples," ASTM STP 632, American Society for Testing and Materials, 1977, pp. 39-56.
5. A. C. Ugural and S. K. Fenster, Advanced Strength and Applied Elasticity, American Elsevier, New York, 1975, p. 83.
6. I. N. Gifford, Jr., "APES - Second Generation Two-Dimensional Fracture Mechanics and Stress Analysis by Finite Elements," Report 4799, Naval Ship Research and Development Center, 1975.
7. M. A. Hussain, S. L. Pu, J. D. Vasilakis, and G. P. O'Hara, Journal of Pressure Vessel Technology, Vol. 102, No. 3, 1980, p. 314.
8. S. L. Pu and M. A. Hussain, Journal of Pressure Vessel Technology, Vol. 103, May 1981, p. 301.

9. H. S. Reemsnyder, "Constant Amplitude Fatigue Life Assessment Models," SAE Technical Paper Series 820688, Proceedings of the SAE Fatigue Conference, April 1982, pp. 119-132.

TABLE I. STRESS ANALYSIS RESULTS

Conditions: $2b_1 = 8.75$ in. (222.3 mm); $2b_2 = 8.41$ in. (213.6 mm)
 $2a = 5.165$ in. (131.2 mm); $P_1 = 72$ ksi (496.4 MPa); $\sigma_{ys} = 180$ ksi (1241 MPa)
 100% overstrain; Specimen dimensions: $X = 6$ in. (152.4 mm); $B = 2.0$ in. (50.8 mm)
 $P =$ Applied compressive force

Equations: Pressure $\sigma_{nom} = \frac{2I_1 a^2}{b_2^2 - a^2} = 87.1$ ksi

Autofrettage $\sigma_{nom} = \sigma_{ys} \left(1 - \frac{2a^2 \ln(b_2 - a)}{b_2^2 - a^2}\right) = 73.8$ ksi

Specimen $\sigma_{nom} = \frac{P}{B(b_2 - a)} \left(\frac{6X}{b_2 - a} - 1\right) = 6.53 P$ (ksi)

Root Radius (in.)	Pressure (ksi)	k_t	Autofrettage (ksi)	k_t	Specimens $(\sigma/P)(in.^{-2})$	k_t	k_t Neuber	Average or Corrected k_t
0.010	509.7	5.85	386.5	5.24	32.74	5.01	6.06	5.37
0.012							5.59	4.95
0.016							4.94	4.38
0.018							4.64	4.11
0.020							4.47	3.96

one inch = 2.54 cm
 one ksi = 6.89 MPa

TABLE II. ESTIMATED LIFE USING LOCAL STRAIN ANALYSIS

$\sigma_u = 190 \text{ ksi (1310 MPa)}$, $\sigma_{\max} - \sigma_{\min} = 87.1 \text{ ksi (600 MPa)}$,
 $E = 30,800 \text{ ksi (212.3 GPa)}$

Root Radius (in.)	k_t	$q(\text{Eq. 4})$	k_f	$\Delta\epsilon(\text{Eq. 2})$	N_f (Cycle) (Fig. 4)
0.010	5.37	0.81	4.54	0.0128	1292
0.012	4.95	0.84	4.32	0.0122	1756
0.016	4.38	0.87	3.94	0.0111	2268
0.018	4.11	0.88	3.73	0.0105	2387
0.020	3.96	0.89	3.63	0.0103	2644

TABLE III. MEASURED LIVES USING THE SIMULATION SPECIMEN

$\Delta K = 50.5 \text{ ksi}\sqrt{\text{in.}}$ ($55.5 \text{ MPa}\sqrt{\text{m}}$) (Average), $R = 0.46$
 $dc/dN = 2.1 \times 10^{-4} \text{ in./cycle}$ ($5.3 \times 10^{-6} \text{ m/cycle}$) (Figure 5)

Specimen	Condition	$\rho(\text{in.})$		$\Delta c(\text{in.})$	N_f (Cycles)	$N_{\Delta c}$ (Cycles)	N_1 (Cycles)
		Before EP	After EP				
1	EP	0.0125	0.0133	.012	2000	57	1943
2	EP	0.0115	0.0125	.034	5000	162	4838
3	EP	0.0135	0.0148	.035	3500	167	3333
7	AM	0.010		.025	2000	119	1883
8	AM	0.015		.012	4000	57	3943
9	AM	0.018		.016	5000	76	4924
10	AM	0.0125		.042	2250	200	2050
15	GP	0.0118		.016	1500	76	1424
21	GP	0.0125		.055	3000	262	2738
22	GP	0.0125		.012	1800	57	1743
17	AM	0.0148		.070	2400	333	2067
18	AM	0.0118		.050	1650	238	1412
24	AM	0.0094		.040	2000	190	1809
25	AM	0.0109		.040	2000	190	1809
28	EP		0.0133	.040	2250	190	2060

Legend EP: Electropolished
 GP: Glass Peened
 AM: As-Machined
 one inch: 25.4 mm

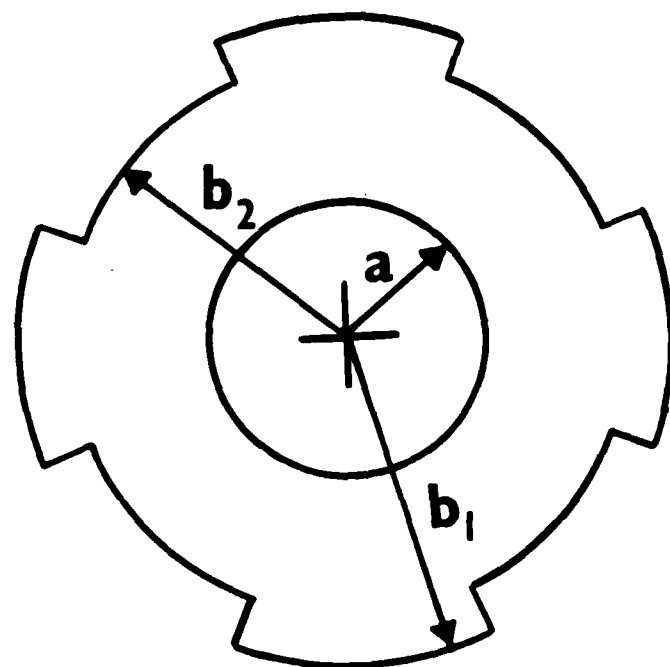


Figure 1. Sectored thread end connection geometry.

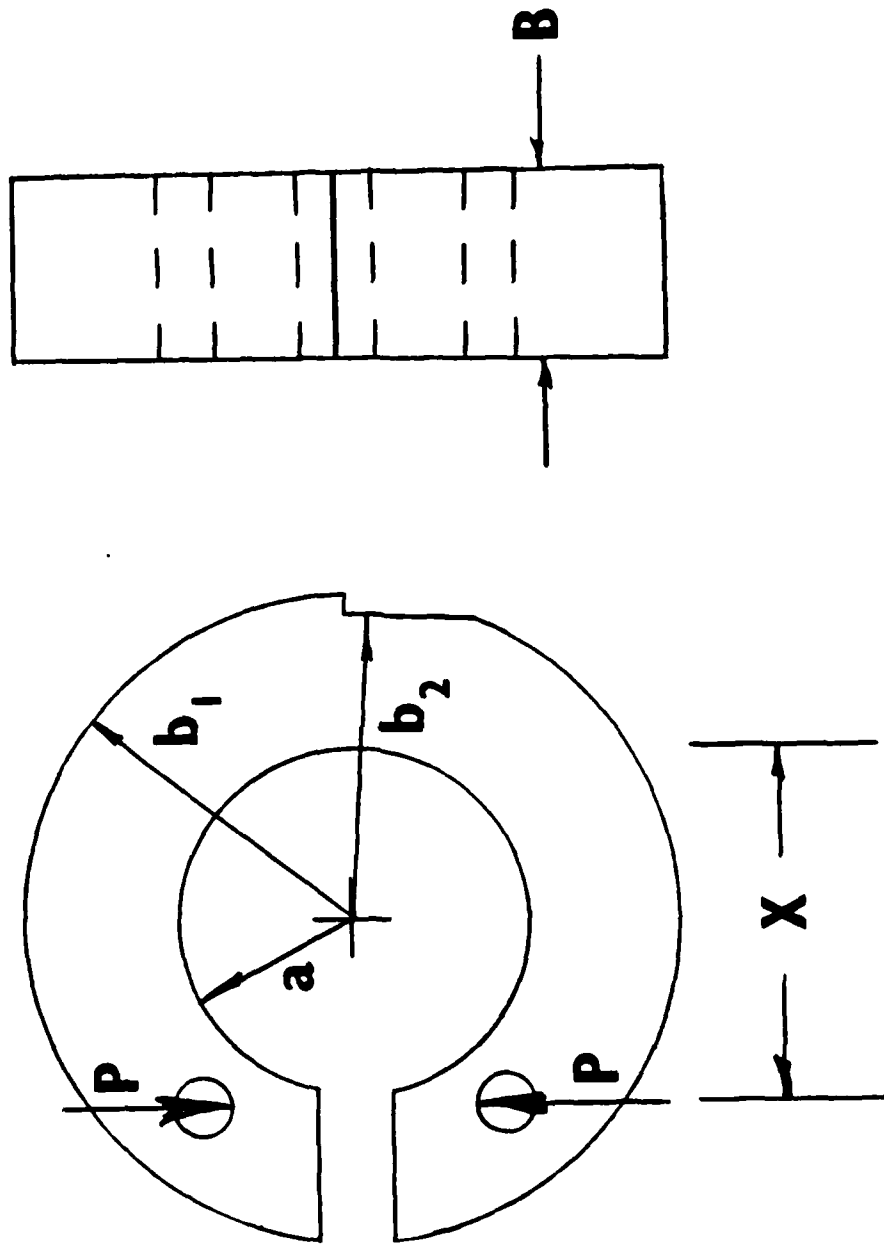
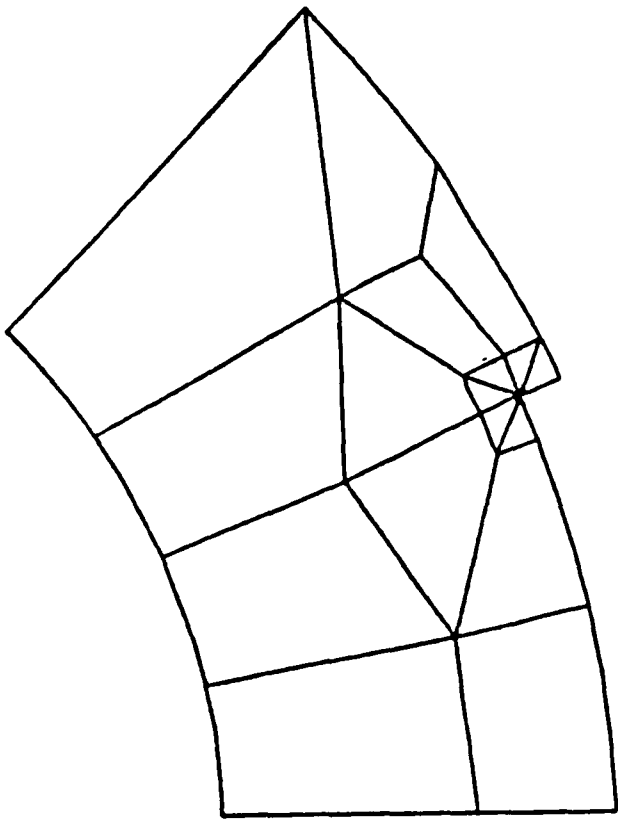
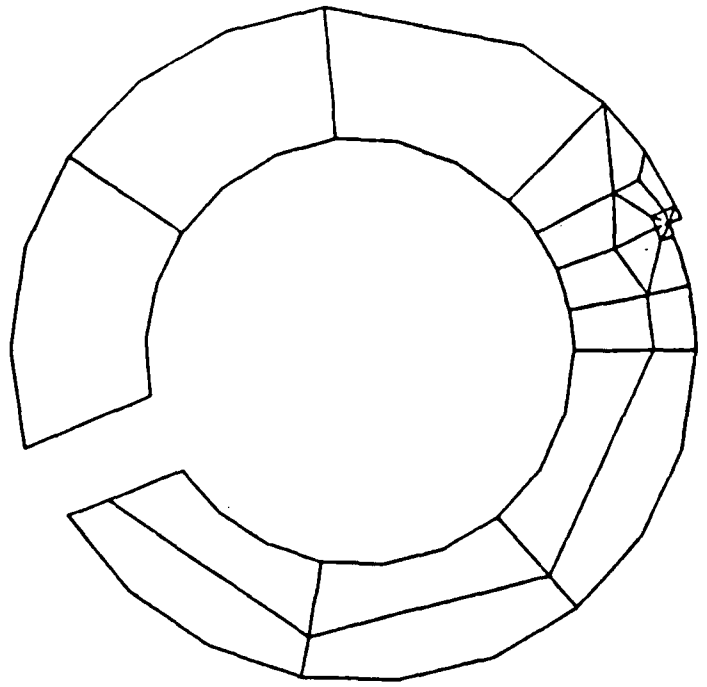


Figure 2. Simulation specimen.

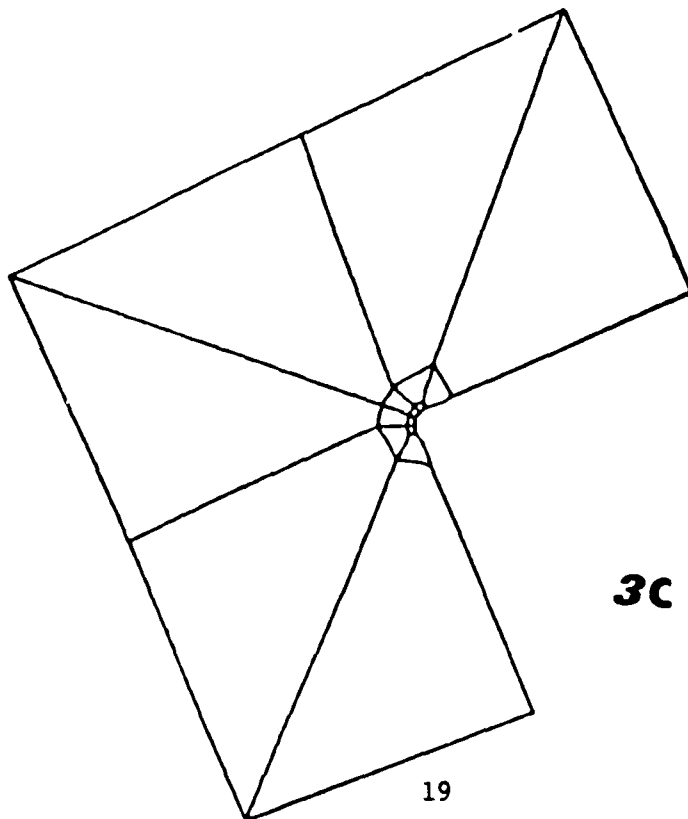


3 a

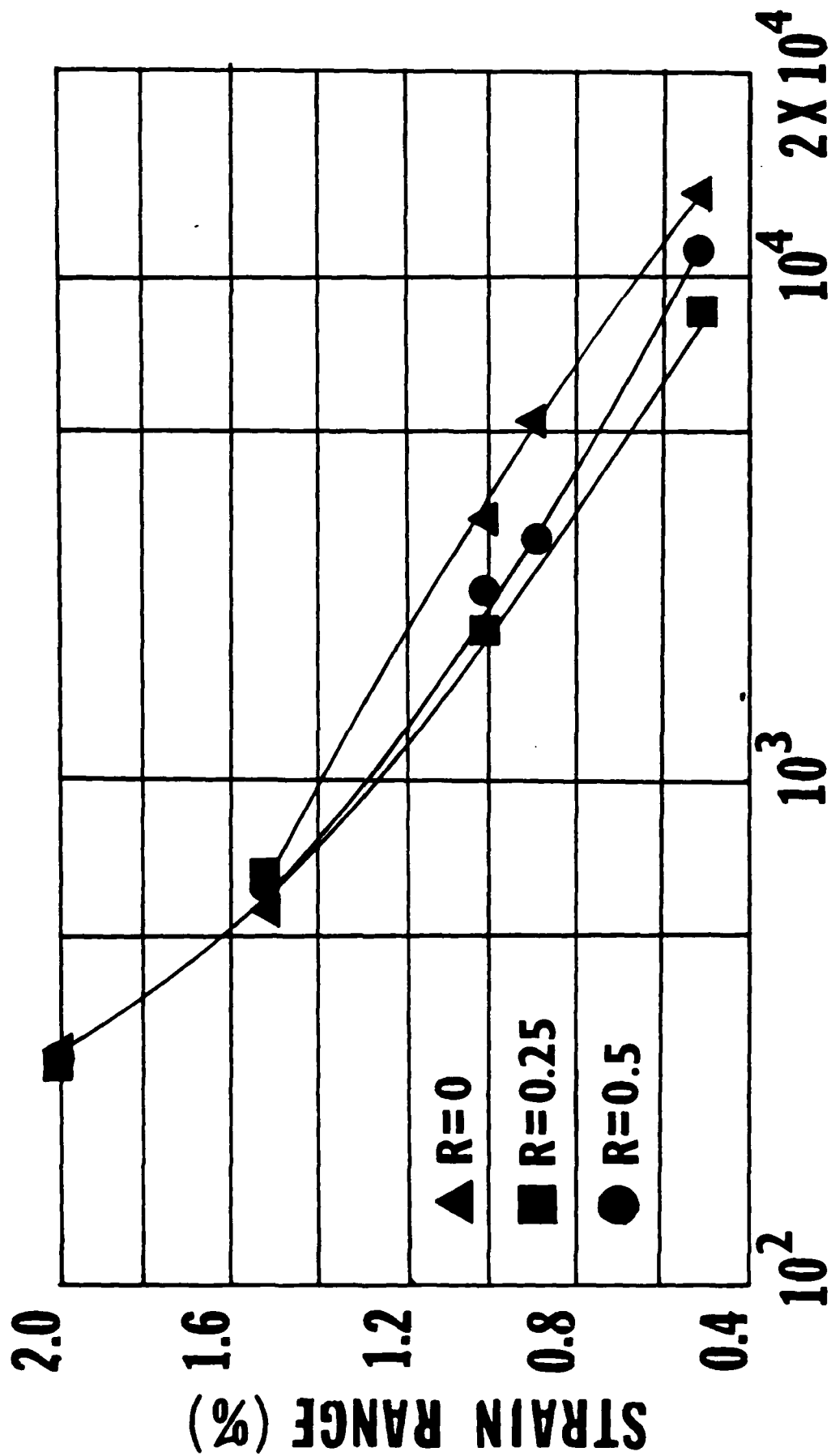


3 b

Figure 3. Finite element models.



3 c



CYCLES

Figure 4. Strain-life property of the steel tested.

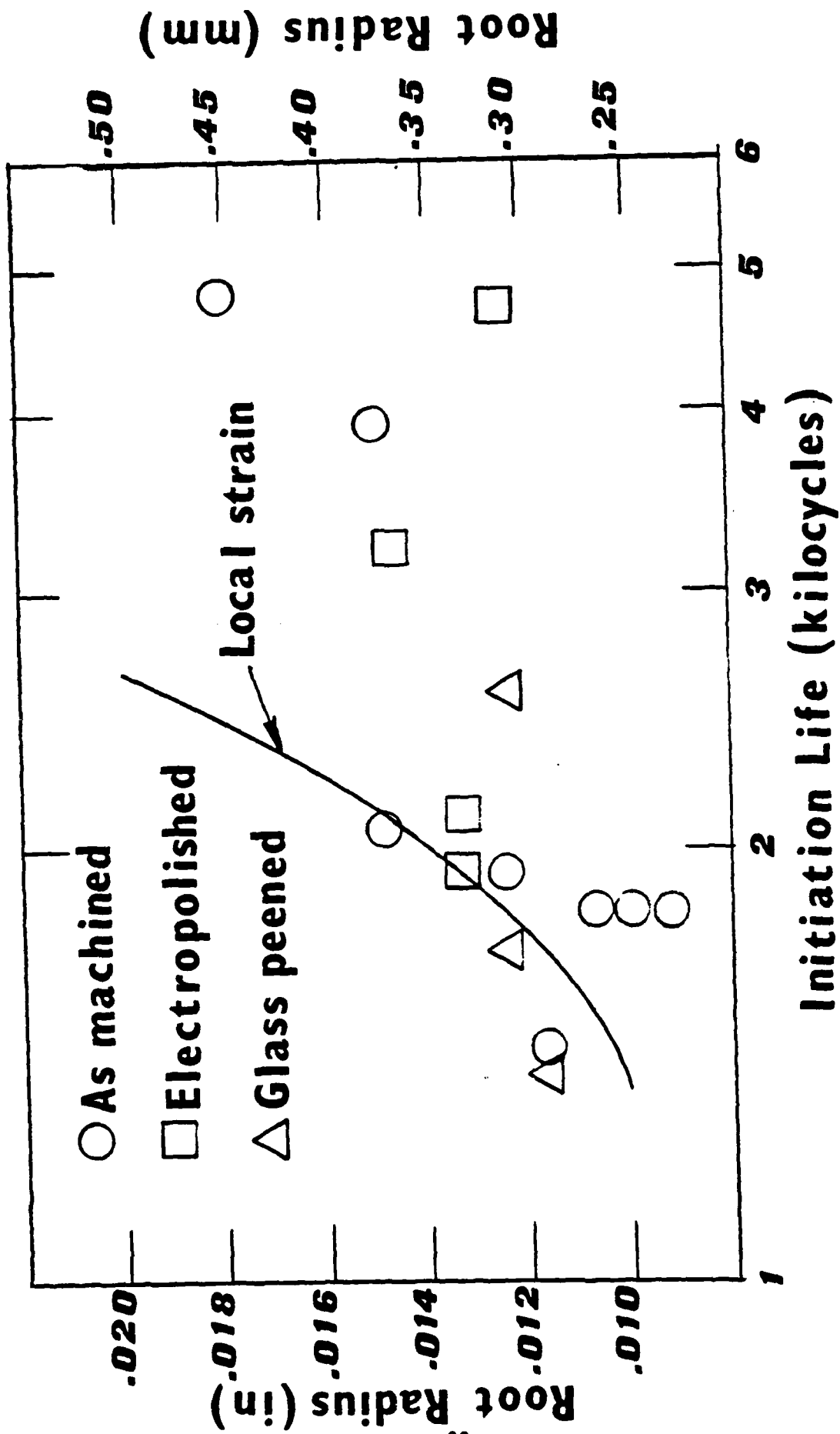


Figure 6. Measured crack initiation life as a function of notch root radius.

TECHNICAL REPORT INTERNAL DISTRIBUTION LIST

	<u>NO. OF COPIES</u>
CHIEF, DEVELOPMENT ENGINEERING BRANCH	
ATTN: SMCAR-CCB-D	1
-DA	1
-DP	1
-DR	1
-DS (SYSTEMS)	1
-DC	1
-DM	1
 CHIEF, ENGINEERING SUPPORT BRANCH	
ATTN: SMCAR-CCB-S	1
-SE	1
 CHIEF, RESEARCH BRANCH	
ATTN: SMCAR-CCB-R	2
-R (ELLEN FOGARTY)	1
-RA	1
-RM	1
-RP	1
-RT	1
 TECHNICAL LIBRARY	
ATTN: SMCAR-CCB-TL	5
 TECHNICAL PUBLICATIONS & EDITING UNIT	
ATTN: SMCAR-CCB-TL	2
 DIRECTOR, OPERATIONS DIRECTORATE	1
 DIRECTOR, PROCUREMENT DIRECTORATE	1
 DIRECTOR, PRODUCT ASSURANCE DIRECTORATE	1

NOTE: PLEASE NOTIFY DIRECTOR, BENET WEAPONS LABORATORY, ATTN: SMCAR-CCB-TL, OF ANY ADDRESS CHANGES.

TECHNICAL REPORT EXTERNAL DISTRIBUTION LIST

	<u>NO. OF COPIES</u>		<u>NO. OF COPIES</u>
ASST SEC OF THE ARMY RESEARCH & DEVELOPMENT ATTN: DEP FOR SCI & TECH THE PENTAGON WASHINGTON, D.C. 20315	1	COMMANDER US ARMY AMCCOM ATTN: SMCAR-ESP-L ROCK ISLAND, IL 61299	1
COMMANDER DEFENSE TECHNICAL INFO CENTER ATTN: DTIC-DDA CAMERON STATION ALEXANDRIA, VA 22314	12	COMMANDER ROCK ISLAND ARSENAL ATTN: SMCRI-ENM (MAT SCI DIV) ROCK ISLAND, IL 61299	1
COMMANDER US ARMY MAT DEV & READ COMD ATTN: DRCDE-SG 5001 EISENHOWER AVE ALEXANDRIA, VA 22333	1	DIRECTOR US ARMY INDUSTRIAL BASE ENG ACTV ATTN: DRXIB-M ROCK ISLAND, IL 61299	1
COMMANDER ARMAMENT RES & DEV CTR US ARMY AMCCOM ATTN: SMCAR-FS SMCAR-FSA SMCAR-FSM SMCAR-FSS SMCAR-AEE SMCAR-AES SMCAR-AET-O (PLASTECH) SMCAR-MSI (STINFO) DOVER, NJ 07801	1 1 1 1 1 1 1 2	COMMANDER US ARMY TANK-AUTMV R&D COMD ATTN: TECH LIB - DRSTA-TSL WARREN, MI 48090	1
DIRECTOR BALLISTICS RESEARCH LABORATORY ATTN: AMXBR-TSB-S (STINFO) ABERDEEN PROVING GROUND, MD 21005	1	COMMANDER US ARMY TANK-AUTMV COMD ATTN: DRSTA-RC WARREN, MI 48090	1
MATERIEL SYSTEMS ANALYSIS ACTV ATTN: DRXSY-MP ABERDEEN PROVING GROUND, MD 21005	1	COMMANDER US MILITARY ACADEMY ATTN: CHMN, MECH ENGR DEPT WEST POINT, NY 10996	1
		US ARMY MISSILE COMD REDSTONE SCIENTIFIC INFO CTR ATTN: DOCUMENTS SECT, BLDG. 4484 REDSTONE ARSENAL, AL 35898	2
		COMMANDER US ARMY FGN SCIENCE & TECH CTR ATTN: DRXST-SD 220 7TH STREET, N.E. CHARLOTTESVILLE, VA 22901	1

NOTE: PLEASE NOTIFY COMMANDER, ARMAMENT RESEARCH, DEVELOPMENT, AND ENGINEERING CENTER, US ARMY AMCCOM, ATTN: BENET WEAPONS LABORATORY, SMCAR-CCB-TL, WATERVLIET, NY 12189-4050, OF ANY ADDRESS CHANGES.

TECHNICAL REPORT EXTERNAL DISTRIBUTION LIST (CONT'D)

	<u>NO. OF COPIES</u>		<u>NO. OF COPIES</u>
COMMANDER US ARMY LABCOM MATERIALS TECHNOLOGY LAB ATTN: SLCMT-IML WATERTOWN, MA 01272	2	DIRECTOR US NAVAL RESEARCH LAB ATTN: DIR, MECH DIV CODE 26-27, (DOC LIB) WASHINGTON, D.C. 20375	1 1
COMMANDER US ARMY RESEARCH OFFICE ATTN: CHIEF, IPO P.O. BOX 12211 RESEARCH TRIANGLE PARK, NC 27709	1	COMMANDER AIR FORCE ARMAMENT LABORATORY ATTN: AFATL/DLJ AFATL/DLJG EGLIN AFB, FL 32542	1 1
COMMANDER US ARMY HARRY DIAMOND LAB ATTN: TECH LIB 2800 POWDER MILL ROAD ADELPHIA, MD 20783	1	METALS & CERAMICS INFO CTR BATTELLE COLUMBUS LAB 505 KING AVENUE COLUMBUS, OH 43201	1
COMMANDER NAVAL SURFACE WEAPONS CTR ATTN: TECHNICAL LIBRARY CODE X212 DAHLGREN, VA 22448	1		

NOTE: PLEASE NOTIFY COMMANDER, ARMAMENT RESEARCH, DEVELOPMENT, AND ENGINEERING CENTER, US ARMY AMCCOM, ATTN: BENET WEAPONS LABORATORY, SMCAR-CCB-TL, WATERVLIET, NY 12189-4050, OF ANY ADDRESS CHANGES.

END

DTIC

8-86